ISSN 0023-1584, Kinetics and Catalysis, 2009, Vol. 50, No. 5, pp. 617–626. © Pleiades Publishing, Ltd., 2009.
Original Russian Text © Yu.K. Karasevich, 2009, published in Kinetika i Kataliz, 2009, Vol. 50, No. 5, pp. 643–652.

Kinetics of Chemical Ionization in Shock Waves: IV. Kinetic Model of Ionization in Acetylene Oxidation

Yu. K. Karasevich

Semenov Institute of Chemical Physics, Russian Academy of Sciences, Moscow, 119991 Russia
e-mail: yukarasevich@yandex.ru

Received May 12, 2008

Abstract—A kinetic model is suggested for chemical ionization in acetylene combustion. The kinetic scheme of the process is obtained by adding the block of reactions responsible for ionization to the acetylene combustion scheme. The results of numerical calculations of the ionization kinetics are compared with experimental data obtained using a microwave interferometer and with ignition delay data available from the literature.

DOI: 10.1134/S0023158409050024

In our earlier work [1], the kinetic simulation of chemical ionization in methane oxidation in a shock wave was based on electron concentration profile measurements with a microwave interferometer. The base methane oxidation mechanism was the mechanism suggested in [2]. The mechanism of chemical ionization in methane flames was based on the following sequence of reactions [3, 4]:

$$CH + O \longrightarrow CHO^+ + e^-,$$

$$CHO^+ + H_2O \longrightarrow H_3O^+ + CO,$$

$$H_3O^+ + e^- \longrightarrow H_2O + H.$$

The results of numerical calculations of the ionization kinetics in methane oxidation are in qualitative agreement with the observed time variation of the electron concentration, thus validating the conception of chemical ionization in hydrocarbon combustion underlying the kinetic scheme. The purpose of this work is to develop a kinetic model for ionization in acetylene combustion based on earlier results [1].

EXPERIMENTAL

The ionization kinetics of some hydrocarbons, including acetylene, was studied earlier using a microwave interferometer [5]. Table 1 lists the mixture compositions examined in the experiments on acetylene. For each mixture, we indicate the temperature range in which the experiments were done and the oxygen excess factor (α). The diluent gas was argon. The gas pressure behind the reflected shock wave was 760 ± 150 Torr in all runs.

We measured the electron concentration as a function of time, $n_e(t)$, and, from these data, derived the following characteristic parameters of the process: maximum ionization rate (W_{max}), induction period (τ_i), maximum concentration time (τ_{max}), and maximum electron yield per carbon atom ($\eta_{max} = n_{max}/n_C$, where $n_C = 2n^0_{C_2H_2}$ and $n^0_{C_2H_2}$ is the initial acetylene concentration in the mixture behind the reflected shock wave). Figure 1 shows examples of electron concentration profiles obtained for two different mixtures at similar temperatures. The characteristic parameters of these profiles as a function of temperature and of the initial acetylene concentration behind the front of the reflected shock wave are presented in Figs. 2–4. Regression analysis of these curves [5] led to the following relationships (the activation energies are in cal/mol):

$$\tau_i = 3.49 \times 10^6 n_C^{-0.8} \exp(19500/RT), \quad (1)$$

$$\tau_{max} = 2.19 \times 10^7 n_C^{-0.8} \exp(15600/RT), \quad (2)$$

$$W_{max} = 1.05 \times 10^9 n_C^{1.65} \exp(-24000/RT), \quad (3)$$

$$\eta_{max} = 9.33 \times 10^{-5} \exp(-13250/RT). \quad (4)$$

In Figs. 2–4, relationships (1)–(4) are plotted as solid lines.

Table 1. Mixture compositions examined in the experimental study of the ionization kinetics in acetylene oxidation

Entry	$[C_2H_2]$, %	$[O_2]$, %	T, K	α
1	0.52	2.43	1340–2530	1.87
2	0.51	1.64	1540–2930	1.29
3	0.26	0.74	1670–2970	1.14
4	0.28	1.26	1250–2910	1.80
5	0.27	0.67	1540–2810	0.99
6	0.27	1.40	2220–3070	2.07

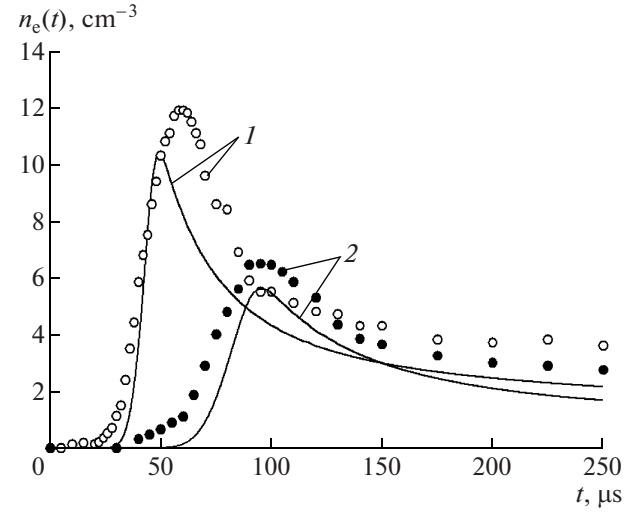

Fig. 1. Calculated (solid lines) and experimental (points) electron concentration profiles for acetylene oxidation: (*1*) mixture 6, $T = 2057$ K; (*2*) mixture 3, $T = 2061$ K.

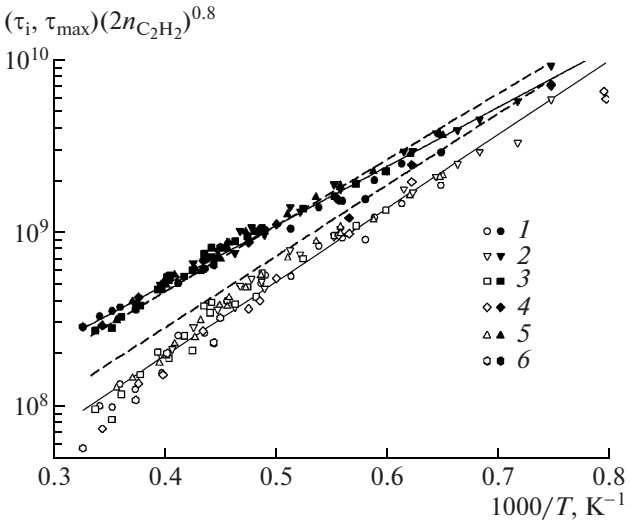

Fig. 2. Arrhenius plots of the ionization induction period (light symbols) and the maximum electron concentration time (dark symbols) in acetylene oxidation. The points are numbered in the same way as the mixtures in Table 1. The solid lines represent τ_i and τ_{max} data calculated using formulas (1) and (2), respectively, and the dashed lines represent the same data calculated using the kinetic scheme. The τ_i and τ_{max} values are in s^{-1}; the $n_{C_2H_2}$ values, in cm^{-3}.

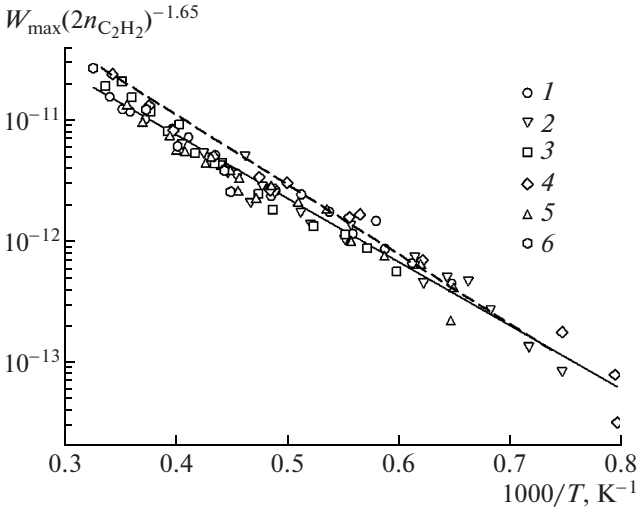

Fig. 3. Arrhenius plots of the maximum ionization rate in acetylene oxidation. The points are numbered in the same way as the mixtures in Table 1. The solid line represents the ionization rate data calculated using formula (3), and the dashed line represents the same data calculated using the kinetic scheme. The W_{max} values are in cm^{-3} s^{-1}; the $n_{C_2H_2}$ values, in cm^{-3}.

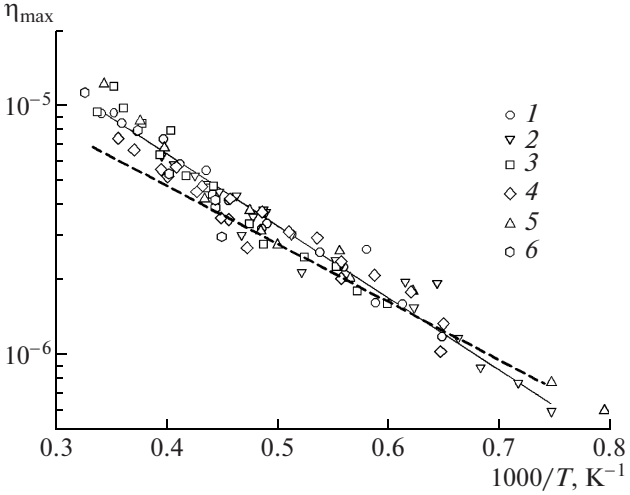

Fig. 4. Arrhenius plots of the electron yield in acetylene oxidation. The points are numbered in the same way as the mixtures in Table 1. The solid line represents the ionization rate data calculated using formula (4), and the dashed line represents the data calculated using the kinetic scheme.

KINETIC MODEL OF ACETYLENE IONIZATION

For the description of the ionization kinetics in acetylene oxidation, we chose the acetylene combustion scheme suggested in [6] as the base mechanism. This kinetic scheme of high-temperature acetylene oxidation is based on known constants of the key elementary reactions. The scheme is in satisfactory agreement with experimental data available on acetylene ignition in wide ranges of temperature (980–2400 K), pressure (0.01–1.0 MPa), and volumetric acetylene concentration (0.5–20.3%).

In an earlier kinetic simulation of chemical ionization in methane oxidation in a shock wave, we determined the block of reactions governing the formation of electron concentration profiles. These reactions were added to the acetylene combustion scheme [6].

The CH radical formation and disappearance reactions were excluded from the block for the reason that they are present in the acetylene combustion scheme. Table 2 presents the complete scheme of ionization in acetylene oxidation. The rate constants of reverse reactions were calculated using thermochemical data [21, 56]. In order to take into account that the decomposition of some multiatomic molecules and radicals takes place in the transition pressure range, the rate constants of these reactions were calculated as suggested in [13]:

$$k = \frac{k_0 k_\infty [\mathrm{M}]}{k_0 [\mathrm{M}] + k_\infty} F,$$

where k_0 and k_∞ are the monomolecular decomposition rate constants in the low- and high-pressure limits (cm^3/s) and [M] is the buffer gas concentration (cm^{-3}).

The correction factor F in the Lindemann formula for the rate constant in the transition pressure range was determined as follows:

$$\log F = \frac{\log F_C}{1 + \left[\frac{\log(k_0[\mathrm{M}]/k_\infty)}{N}\right]^2},$$

where $N = 0.75 - 1.27\log F_C$ and $F_C = a\exp(-T/T_1) + \exp(-T_2/T) + (1 - a)\exp(-T/T_3)$. The parameters a, T_1, T_2, and T_3 are listed in Table 2.

Note that the block of reaction responsible for ionization does not exert any significant effect on the parameters of the main combustion process. This was ascertained by relevant calculations.

CALCULATED DATA

Figure 1 shows electron concentration profiles calculated for the conditions under which the experimental profiles plotted in this figure were obtained. According to the calculations, ionization develops as follows. Initially, the CHO^+ ion forms via reaction (196) (Table 2). The rapid recharging process (197) yields the H_3O^+ ion, whose concentration is low at the early stages of the process and is approximately equal to the electron concentration over most of the process development time. After reaching a maximum, which nearly coincides in time with the completion of acetylene oxidation, the H_3O^+ and electron concentrations begin to decreases because of the recombination reaction (198). This is accompanied by an increase in the concentration of Na^+ ions, which result from reactions (200)–(202) at a comparatively low rate.

From Fig. 1, one can judge the fit between the calculated and experimental data. A deeper insight can be gained by comparing the calculated dependences of electron concentration profile parameters (Figs. 2–4, dashed lines) with experimental data.

RESULTS AND DISCUSSION

Note the difference between the calculated and experimental dependences. The calculated characteristic times τ_i and ionization rates somewhat exceed the respective experimental values, and the calculated electron yields are higher than the experimental ones. There are also differences between the slopes of the calculated and experimental dependences in the Arrhenius coordinates.

The start of the intensive growth of the electron concentration coincides with the beginning of the active stage of combustion. Therefore, the characteristic induction time of ionization and the ignition delay time have the same physical meaning. Let us compare these characteristic times. To do this, we will use the τ_i data obtained in this study and the ignition delay data from [6, 57]. Our previous experiments on the ignition of $C_2H_2/O_2/Ar$ mixtures [6] were carried out at T = 980–1300 K and P = 4900 ± 375 Torr. The 20.3% C_2H_2 + 16.7% O_2, 7.75% C_2H_2 + 19.38% O_2, and 2.72% C_2H_2 + 20.4% O_2 mixtures were studied. The ignition delay was taken to be equal to the time interval between the arrival of the shock wave at the end of the tube and a 10% increase in pressure at the tube end. In another work [57], the ignition point was taken to coincide with the beginning of a sharp increase in the light emission intensity and experiments were performed at T = 1300–2400 K and P = 75.0 ± 37.5 Torr. $C_2H_2/O_2/Ar$ mixtures were studied in that work, which contained 0.57% C_2H_2 + 4.43% O_2, 2.9% C_2H_2 + 2.1% O_2, or 2% C_2H_2 + 3% O_2. In our experiments, the mixture pressure was 760 ± 150 Torr. The mixture compositions and temperature ranges are listed in Table 1.

Clearly, the temperature ranges examined by different authors overlap and the pressures examined vary widely. As a consequence, the limiting values of the absolute acetylene concentration differ by nearly 4 orders of magnitude and the total density varies by a factor of ~300. To unify the data from different sources, we use the relationship between τ_i and the acetylene concentration (Eq. (1)) and estimate the dependence of τ_i on the total pressure by minimizing the correlation coefficient in regression analysis. Finally, we obtain $\tau \sim n_C^{-0.8} n_M^{-1/3}$, where n_M is the total density (cm^{-3}). Figure 5 represents the experimental data in the corresponding coordinate systems. It can readily be seen that data points from different sources, obtained at essentially different pressures and mixture compositions, are describable in terms of a single relationship. The solid third-order curve was obtained by regression analysis of experimental data (the correlation coefficient is 0.986).

Using the acetylene combustion scheme reported in [6], we also carried calculations in which the initial conditions were adjusted to the conditions of the above-mentioned experiments. In these calculations, the ignition time was taken to be equal to the time indicated by the intersection between the tangent to

Table 2. Kinetic scheme of ionization in acetylene oxidation (with rate constants expressed in terms of cm^{-3}, s, kcal/mol)

Entry	Reaction	A	n	E	Reference
1	$C_2H_2 + M \rightleftharpoons C_2H + H + M$	6.03×10^{-8}	0	108.00	[7]
2	$C_2H_2 + H\ (+M) \rightleftharpoons C_2H_3\ (+M)$	6.04×10^{-14}	1.1	2.64	k_∞ [8]
		6.20×10^{-8}	−7.269	6.58	k_0 [9]
	$a = 0.7507,\ T_1 = 1302,\ T_2 = 4167,\ T_3 = 98.5$				[10]
3	$C_2H_2 + C_2H_2 \rightleftharpoons iC_4H_3 + H$	1.88×10^{-10}	0	56.00	[11]
4	$C_2H_2 + C_2H_3 \rightleftharpoons C_4H_4 + H$	3.30×10^{-12}	0	5.00	[11]
5	$C_2H_2 + C_2H \rightleftharpoons nC_4H_3$	1.30×10^{-10}	0	0.084	[12]
6	$C_2H_2 + C_2H \rightleftharpoons C_4H_2 + H$	1.48×10^{-10}	0	0.00	[13]
7	$C_2H_2 + CH_3 \rightleftharpoons aC_3H_4 + H$	1.12×10^{-4}	−2.1	31.59	[14]
8	$C_2H_2 + CH_3 \rightleftharpoons pC_3H_4 + H$	3.17×10^{-20}	2.4	12.90	[15]
9	$C_2H_2 + CH_2 \rightleftharpoons pC_3H_4$	6.92×10^{-12}	0	6.62	[11]
10	$C_2H_2 + CH_2 \rightleftharpoons C_3H_3 + H$	1.99×10^{-11}	0	6.62	[16]
11	$C_2H_2 + CH \rightleftharpoons C_3H_2 + H$	4.98×10^{-11}	0	0.00	[16]
12	$C_2H_2 + HO_2 \rightleftharpoons CH_2CO + OH$	1.00×10^{-14}	0	7.95	[17]
13	$C_2H_2 + O_2 \rightleftharpoons C_2H + HO_2$	1.99×10^{-11}	0	74.52	[17]
14	$C_2H_2 + O_2 \rightleftharpoons CH_2 + CO_2$	7.64×10^{-9}	−0.5	45.00	[18]
15	$C_2H_2 + OH \rightleftharpoons C_2H + H_2O$	5.63×10^{-17}	2.0	14.00	[19]
16	$C_2H_2 + OH \rightleftharpoons CH_2CO + H$	1.83×10^{-11}	0	7.17	[20]
17	$C_2H_2 + OH \rightleftharpoons CH_3 + CO$	8.14×10^{-28}	4.0	−2.00	[19]
18	$C_2H_2 + O \rightleftharpoons CH_2 + CO$	3.45×10^{-10}	0	9.90	[11]
19	$C_2H_2 + O \rightleftharpoons HCCO + H$	8.63×10^{-10}	0	10.70	[11]
20	$C_2H_2 + H \rightleftharpoons C_2H + H_2$	1.00×10^{-10}	0	27.82	[21]
21	$C_2H_4\ (+M) \rightleftharpoons C_2H_2 + H_2\ (+M)$	8.00×10^{12}	0.4	88.77	k_∞ [10]
		1.16×10^{27}	−9.31	99.86	k_0 [10]
	$a = 0.7345,\ T_1 = 1035,\ T_2 = 5417,\ T_3 = 180$				[10]
22	$C_2H_4 + OH \rightleftharpoons C_2H_3 + H_2O$	3.40×10^{-11}	0	5.94	[21]
23	$C_2H_4 + O \rightleftharpoons C_2H_3 + OH$	6.61×10^{-10}	0	18.88	[22]
24	$C_2H_4 + O \rightleftharpoons CH_2CHO + H$	1.13×10^{-12}	0	0.70	[11]
25	$C_2H_4 + O \rightleftharpoons CH_2CO + H_2$	1.12×10^{-18}	1.9	0.18	[13]
26	$C_2H_4 + H\ (+M) \rightleftharpoons C_2H_5\ (+M)$	1.79×10^{-12}	0.5	1.82	k_∞ [10]
		3.31×10^{-6}	−7.62	6.97	k_0 [10]
	$a = 0.9753,\ T_1 = 987,\ T_2 = 4374,\ T_3 = 210$				[10]
27	$C_2H_4 + H \rightleftharpoons C_2H_3 + H_2$	8.92×10^{-10}	0	14.90	[21]
28	$C_2H_3 + H\ (+M) \rightleftharpoons C_2H_4\ (+M)$	1.01×10^{-11}	0.3	0.28	k_∞ [10]
		3.86×10^{-18}	−3.86	3.32	k_0 [10]
	$a = 0.782,\ T_1 = 2663,\ T_2 = 6095,\ T_3 = 207.5$				[10]
29	$C_2H_3 + C_2H_3 \rightleftharpoons C_4H_4 + H + H$	1.30×10^{-11}	0	0	[23]
30	$C_2H_3 + C_2H \rightleftharpoons C_2H_2 + C_2H_2$	1.66×10^{-12}	0	0	[17]
31	$C_2H_3 + O_2 \rightleftharpoons C_2H_2 + HO_2$	7.42×10^{-19}	1.6	−0.38	[6]
32	$C_2H_3 + O_2 \rightleftharpoons CH_2O + HCO$	1.52×10^{-8}	−1.4	1.01	[6]
33	$C_2H_3 + O_2 \rightleftharpoons CH_2CHO + O$	2.01×10^{-12}	−0.3	0.01	[6]
34	$C_2H_3 + O \rightleftharpoons CH_2CO + H$	1.59×10^{-10}	0	0	[17]
35	$C_2H_3 + H \rightleftharpoons C_2H_2 + H_2$	1.99×10^{-11}	0	0	[16]
36	$C_2H_3 + OH \rightleftharpoons C_2H_2 + H_2O$	5.25×10^{-11}	0	0	[16]

Table 2. (Contd.)

Entry	Reaction	A	n	E	Reference
37	$nC_4H_3 \rightleftharpoons iC_4H_3$	4.10×10^{43}	−9.5	53.00	[16]
38	$iC_4H_3 + O_2 \rightleftharpoons HCCO + CH_2CO$	1.30×10^{-7}	−1.8	0	[16]
39	$nC_4H_3 + H \rightleftharpoons C_4H_2 + H_2$	4.98×10^{-11}	0	0	[16]
40	$iC_4H_3 + H \rightleftharpoons C_4H_2 + H_2$	9.96×10^{-11}	0	0	[16]
41	$C_4H_2 + H \rightleftharpoons nC_4H_3$	1.83×10^{18}	−8.7	15.30	[16]
42	$C_4H_2 + H \rightleftharpoons iC_4H_3$	1.83×10^{6}	−4.9	10.80	[16]
43	$C_4H_2 + O \rightleftharpoons C_3H_2 + CO$	4.48×10^{-11}	0	1.72	[16]
44	$C_4H_2 + OH \rightleftharpoons C_4H + H_2O$	5.60×10^{-17}	2.0	14.00	[16]
45	$C_4H + H\ (+M) \rightleftharpoons C_4H_2\ (+M)$	1.66×10^{-7}	−1	0	k_∞ [16]
		1.03×10^{-14}	−4.8	1.90	k_0 [16]
	$a = 0.6464,\ T_1 = 1315,\ T_2 = 5566,\ T_3 = 132$				[10]
46	$C_4H + O \rightleftharpoons C_2H + C_2O$	8.30×10^{-11}	0	0	[16]
47	$C_4H + O_2 \rightleftharpoons HCCO + C_2O$	8.30×10^{-11}	0	1.50	[16]
48	$C_4H + H_2 \rightleftharpoons C_4H_2 + H$	8.14×10^{-19}	2.5	0.56	[16]
49	$pC_3H_4 \rightleftharpoons aC_3H_4$	5.15×10^{60}	−13.9	91.12	[16]
50	$aC_3H_4 + H \rightleftharpoons C_3H_3 + H_2$	2.14×10^{-18}	2.0	5.50	[16]
51	$aC_3H_4 + O \rightleftharpoons CH_2CO + CH_2$	3.32×10^{-17}	1.8	1.00	[16]
52	$aC_3H_4 + OH \rightleftharpoons C_3H_3 + H_2O$	8.80×10^{-18}	2.0	2.00	[16]
53	$aC_3H_4 + CH_3 \rightleftharpoons C_3H_3 + CH_4$	3.32×10^{-12}	0	7.70	[16]
54	$aC_3H_4 + C_2H \rightleftharpoons C_2H_2 + C_3H_3$	1.66×10^{-11}	0	0	[16]
55	$pC_3H_4 + H \rightleftharpoons aC_3H_4 + H$	1.04×10^{-6}	−0.9	10.08	[16]
56	$pC_3H_4 + O \rightleftharpoons HCCO + CH_3$	1.20×10^{-11}	0	2.25	[16]
57	$pC_3H_4 + O \rightleftharpoons C_2H_4 + CO$	1.66×10^{-11}	0	2.25	[16]
58	$pC_3H_4 + OH \rightleftharpoons C_3H_3 + H_2O$	1.66×10^{-18}	2.0	0.10	[16]
59	$pC_3H_4 + CH_3 \rightleftharpoons C_3H_3 + CH_4$	3.32×10^{-12}	0	7.70	[11]
60	$pC_3H_4 + C_2H \rightleftharpoons C_2H_2 + C_3H_3$	1.66×10^{-11}	0	0	[16]
61	$C_3H_3 + HO_2 \rightleftharpoons aC_3H_4 + O_2$	3.15×10^{-13}	0	15.00	[16]
62	$C_3H_3 + HO_2 \rightleftharpoons pC_3H_4 + O_2$	5.26×10^{-12}	0	15.00	[16]
63	$C_3H_3 + HCO \rightleftharpoons aC_3H_4 + CO$	4.15×10^{-11}	0	0	[16]
64	$C_3H_3 + HCO \rightleftharpoons pC_3H_4 + CO$	4.15×10^{-11}	0	0	[16]
65	$C_3H_3 + HO_2 \rightleftharpoons C_2H_3 + OH + CO$	1.32×10^{-12}	0	0	[16]
66	$C_3H_3 + CH_2 \rightleftharpoons C_4H_4 + H$	8.30×10^{-11}	0	0	[16]
67	$C_3H_3 + O_2 \rightleftharpoons CH_2CO + HCO$	5.25×10^{-14}	0	2.87	[16]
68	$C_3H_3 + OH \rightleftharpoons C_2H_3 + HCO$	6.61×10^{-11}	0	0	[16]
69	$C_3H_3 + O \rightleftharpoons CH_2O + C_2H$	3.32×10^{-11}	0	0	[16]
70	$C_3H_3 + H\ (+M) \rightleftharpoons aC_3H_4\ (+M)$	3.32×10^{-11}	0	0	k_∞ [16]
		6.31×10^{8}	−12.55	7.934	k_0 [16]
	$a = 0.234,\ T_1 = 4808,\ T_2 = 7262,\ T_3 = 330$				[16]
71	$CH_3CO + M \rightleftharpoons CH_3 + CO + M$	1.45×10^{19}	−8.6	22.42	[17]
72	$CH_3CO + OH \rightleftharpoons CH_2CO + H_2O$	1.99×10^{-11}	0	0	[17]
73	$CH_3CO + H \rightleftharpoons CH_2CO + H_2$	4.17×10^{-11}	0	0	[24]
74	$CH_3CO + O \rightleftharpoons CH_3 + CO_2$	1.66×10^{-11}	0	0	[17]
75	$CH_2CHO \rightleftharpoons CH_3CO$	1.00×10^{13}	0	47.00	[16]
76	$CH_2CHO \rightleftharpoons CH_2CO + H$	1.05×10^{37}	−7.2	44.32	[11]
77	$CH_2CHO + O_2 \rightleftharpoons CH_2O + CO + OH$	3.02×10^{-14}	0	0	[16]

Table 2. (Contd.)

Entry	Reaction	A	n	E	Reference
78	$CH_2CO + M \rightleftharpoons CH_2 + CO + M$	3.80×10^{-9}	0	57.60	[25]
79	$CH_2CO + H \rightleftharpoons CH_3 + CO$	1.86×10^{-17}	2.0	2.00	[11]
80	$CH_2CO + H \rightleftharpoons HCCO + H_2$	3.02×10^{-10}	0	8.60	[11]
81	$CH_2CO + O \rightleftharpoons CH_2 + CO_2$	1.66×10^{-11}	0	0	[26]
82	$CH_2CO + OH \rightleftharpoons CH_2OH + CO$	8.32×10^{-12}	0	0	[26]
83	$CH_2CO + CH_2 \rightleftharpoons CH_3 + HCCO$	6.03×10^{-11}	0	11.00	[26]
84	$CH_2CO + CH_2 \rightleftharpoons C_2H_4 + CO$	1.66×10^{-12}	0	0	[26]
85	$HCCO + M \rightleftharpoons CH + CO + M$	1.07×10^{-8}	0	58.80	[27]
86	$HCCO + C_2H_2 \rightleftharpoons C_3H_3 + CO$	1.66×10^{-13}	0	3.00	[10]
87	$HCCO + CH_2 \rightleftharpoons C_2H + CH_2O$	1.66×10^{-11}	0	2.00	[28]
88	$HCCO + CH_2 \rightleftharpoons C_2H_3 + CO$	5.25×10^{-11}	0	0	[28]
89	$HCCO + O_2 \rightleftharpoons CO + CO + OH$	6.92×10^{-14}	0	0.85	[26]
90	$HCCO + O_2 \rightleftharpoons HCO + CO_2$	1.66×10^{-10}	0	11.50	[21]
91	$HCCO + OH \rightleftharpoons C_2O + H_2O$	5.25×10^{-11}	0	0	[16]
92	$HCCO + H \rightleftharpoons CH_2 + CO$	2.51×10^{-10}	0	0	[27]
93	$HCCO + O \rightleftharpoons CO + CO + H$	1.59×10^{-10}	0	0	[29]
94	$HCCO + O \rightleftharpoons CH + CO_2$	4.90×10^{-11}	0	1.11	[29]
95	$CH_3OH + M \rightleftharpoons CH_3 + OH + M$	5.76×10^{-8}	0	66.44	[30]
96	$CH_3OH + OH \rightleftharpoons CH_2OH + H_2O$	2.41×10^{-18}	2.0	−0.84	[31]
97	$CH_3OH + O \rightleftharpoons CH_2OH + OH$	5.76×10^{-11}	0	5.47	[32]
98	$CH_3OH + H \rightleftharpoons CH_2OH + H_2$	2.69×10^{-17}	2.0	4.52	[31]
99	$CH_3OH + HO_2 \rightleftharpoons CH_2OH + H_2O_2$	1.59×10^{-13}	0	12.58	[17]
100	$CH_2OH + M \rightleftharpoons CH_2O + H + M$	7.26×10^{-9}	0	30.00	[26]
101	$CH_2OH + O_2 \rightleftharpoons CH_2O + HO_2$	1.66×10^{-10}	0	6.00	[33]
102	$CH_2OH + C_2H_2 \rightleftharpoons C_2H_3 + CH_2O$	1.20×10^{-12}	0	9.00	[17]
103	$CH_3O + M \rightleftharpoons CH_2O + H + M$	8.92×10^{-11}	0	13.50	[13]
104	$CH_3O + CH_3O \rightleftharpoons CH_2O + CH_3OH$	1.00×10^{-10}	0	0	[17]
105	$CH_3O + O_2 \rightleftharpoons CH_2O + HO_2$	6.03×10^{-14}	0	2.13	[21]
106	$CH_3O + OH \rightleftharpoons H_2O + CH_2O$	3.02×10^{-11}	0	0	[17]
107	$CH_3O + H \rightleftharpoons H_2 + CH_2O$	3.32×10^{-11}	0	0	[17]
108	$CH_3O + O \rightleftharpoons OH + CH_2O$	1.00×10^{-11}	0	0	[17]
109	$CH_2O + M \rightleftharpoons HCO + H + M$	6.19×10^{-9}	0	73.34	[34]
110	$CH_2O + M \rightleftharpoons CO + H_2 + M$	7.70×10^{-9}	0	65.70	[34]
111	$CH_2O + CH_3 \rightleftharpoons CH_4 + HCO$	9.13×10^{-21}	2.8	5.86	[17]
112	$CH_2O + HO_2 \rightleftharpoons HCO + H_2O_2$	3.32×10^{-12}	0	11.67	[17]
113	$CH_2O + OH \rightleftharpoons HCO + H_2O$	5.76×10^{-15}	1.2	−0.45	[21]
114	$CH_2O + O_2 \rightleftharpoons HCO + HO_2$	3.39×10^{-11}	0	38.95	[17]
115	$CH_2O + H \rightleftharpoons HCO + H_2$	3.80×10^{-14}	1.1	3.28	[21]
116	$CH_2O + O \rightleftharpoons HCO + OH$	6.92×10^{-13}	0.6	2.76	[21]
117	$HCO + M \rightleftharpoons H + CO + M$	1.15×10^{-6}	−1.0	17.00	[26]
118	$HCO + HCO \rightleftharpoons CH_2O + CO$	3.02×10^{-11}	0	0	[17]
119	$HCO + O_2 \rightleftharpoons CO + HO_2$	2.57×10^{-20}	2.4	−1.53	[35]
120	$HCO + OH \rightleftharpoons CO + H_2O$	1.66×10^{-10}	0	0	[21]
121	$HCO + H \rightleftharpoons CO + H_2$	1.51×10^{-10}	0	0	[21]
122	$HCO + O \rightleftharpoons CO + OH$	5.25×10^{-11}	0	0	[21]

Table 2. (Contd.)

Entry	Reaction	A	n	E	Reference
123	$HCO + O \rightleftharpoons H + CO_2$	5.01×10^{-11}	0	0	[21]
124	$CH_3 + CH_3 (+M) \rightleftharpoons C_2H_6 (+M)$	3.52×10^{-8}	−1.0	0.62	k_∞ [10]
		4.88×10^{2}	−9.67	6.22	k_0 [10]
	$a = 0.5325$, $T_1 = 1038$, $T_2 = 4970$, $T_3 = 151$				[10]
125	$C_2H_6 + H \rightleftharpoons C_2H_5 + H_2$	2.41×10^{-15}	1.5	7.41	[21]
126	$C_2H_6 + OH \rightleftharpoons C_2H_5 + H_2O$	1.20×10^{-17}	2.0	0.90	[21]
127	$C_2H_6 + O \rightleftharpoons C_2H_5 + OH$	1.66×10^{-15}	1.5	5.80	[21]
128	$C_2H_5 + H (+M) \rightleftharpoons C_2H_6 (+M)$	8.65×10^{-7}	−1.0	1.58	k_∞ [10]
		5.49×10^{7}	−7.1	6.69	k_0 [10]
	$a = 0.8422$, $T_1 = 2219$, $T_2 = 6882$, $T_3 = 125$				[10]
129	$C_2H_5 + OH \rightleftharpoons C_2H_4 + H_2O$	4.17×10^{-11}	0	0	[17]
130	$C_2H_5 + O_2 \rightleftharpoons C_2H_4 + HO_2$	4.17×10^{-5}	−2.8	1.98	[36]
131	$CH_4 + H \rightleftharpoons CH_3 + H_2$	2.19×10^{-20}	3.0	8.04	[21]
132	$CH_4 + OH \rightleftharpoons CH_3 + H_2O$	2.62×10^{-17}	1.8	2.78	[21]
133	$CH_4 + O \rightleftharpoons CH_3 + OH$	1.15×10^{-15}	1.6	8.49	[21]
134	$CH_3 + H (+M) \rightleftharpoons CH_4 (+M)$	2.11×10^{-8}	−0.6	0.38	k_∞ [11]
		4.11×10^{-15}	−4.8	2.44	k_0 [11]
	$a = 0.783$, $T_1 = 2941$, $T_2 = 6964$, $T_3 = 74$				[11]
135	$CH_3 + M \rightleftharpoons CH_2 + H + M$	3.32×10^{-8}	0	91.40	[37]
136	$CH_3 + M \rightleftharpoons CH + H_2 + M$	1.66×10^{-8}	0	85.25	[38]
137	$CH_3 + CH_2 \rightleftharpoons C_2H_4 + H$	6.92×10^{-11}	0	0	[21]
138	$CH_3 + OH \rightleftharpoons CH_2O + H_2$	5.25×10^{-12}	−0.53	10.81	[14]
139	$CH_3 + O \rightleftharpoons CH_2O + H$	1.41×10^{-10}	0	0	[21]
140	$CH_3 + H \rightleftharpoons CH_2 + H_2$	1.00×10^{-10}	0	15.10	[21]
141	$CH_2 + M \rightleftharpoons CH + H + M$	9.33×10^{-9}	0	89.63	[39]
142	$CH_2 + M \rightleftharpoons C + H_2 + M$	2.62×10^{-10}	0	64.00	[40]
143	$CH_2 + CH_2 \rightleftharpoons C_2H_2 + H + H$	3.32×10^{-10}	0	10.99	[39]
144	$CH_2 + CH_2 \rightleftharpoons C_2H_2 + H_2$	2.62×10^{-9}	0	11.95	[39]
145	$CH_2 + CH_2 \rightleftharpoons C_2H_3 + H$	3.32×10^{-11}	0	0	[22]
146	$CH_2 + O_2 \rightleftharpoons HCO + OH$	2.76×10^{-3}	−3.3	2.87	[41]
147	$CH_2 + O_2 \rightleftharpoons CO_2 + H + H$	8.32×10^{-14}	0	0	[42]
148	$CH_2 + O_2 \rightleftharpoons CO_2 + H_2$	4.37×10^{-3}	−3.3	2.87	[41]
149	$CH_2 + O_2 \rightleftharpoons CO + H_2O$	3.72×10^{-2}	−3.3	2.87	[41]
150	$CH_2 + O_2 \rightleftharpoons CH_2O + O$	5.50×10^{-3}	−3.3	2.87	[41]
151	$CH_2 + OH \rightleftharpoons CH_2O + H$	3.02×10^{-11}	0	0	[17]
152	$CH_2 + OH \rightleftharpoons CH + H_2O$	1.69×10^{-11}	0	0	[10]
153	$CH_2 + O \rightleftharpoons CH + OH$	5.25×10^{-10}	0	11.92	[22]
154	$CH_2 + O \rightleftharpoons CO + H_2$	1.66×10^{-11}	0	0	[22]
155	$CH_2 + O \rightleftharpoons CO + H + H$	1.05×10^{-10}	0	0	[21]
156	$CH_2 + H \rightleftharpoons CH + H_2$	1.32×10^{-11}	0	0	[25]
157	$CH + M \rightleftharpoons C + H + M$	5.25×10^{-10}	0	72.00	[40]
158	$CH + O \rightleftharpoons CO + H$	6.61×10^{-11}	0	0	[21]
159	$CH + H \rightleftharpoons C + H_2$	1.32×10^{-10}	0	0	[43]

Table 2. (Contd.)

Entry	Reaction	A	n	E	Reference
160	$CH + O_2 \rightleftharpoons CO + OH$	8.32×10^{-11}	0	0	[44]
161	$CH + O_2 \rightleftharpoons HCO + O$	1.66×10^{-11}	0	0	[45]
162	$CH + O_2 \rightleftharpoons CO_2 + H$	3.32×10^{-11}	0	0	[11]
163	$CH + CO_2 \rightleftharpoons HCO + CO$	1.66×10^{-12}	0	0	[21]
164	$C_2H + O_2 \rightleftharpoons HCCO + O$	1.00×10^{-12}	0	0	[17]
165	$C_2H + O_2 \rightleftharpoons CO + CO + H$	3.02×10^{-11}	0	0	[11]
166	$C_2H + O_2 \rightleftharpoons HCO + CO$	3.98×10^{-12}	0	0	[17]
167	$C_2H + O \rightleftharpoons CO + CH$	1.66×10^{-11}	0	0	[21]
168	$CO + OH \rightleftharpoons CO_2 + H$	3.55×10^{-12}	0	5.23	[46]
169	$CO + HO_2 \rightleftharpoons CO_2 + OH$	2.51×10^{-10}	0	23.65	[17]
170	$CO + O + M \rightleftharpoons CO_2 + M$	1.70×10^{-33}	0	3.00	[17]
171	$CO_2 + O \rightleftharpoons CO + O_2$	2.82×10^{-11}	0	52.66	[17]
172	$C_2O + H \rightleftharpoons CH + CO$	8.32×10^{-11}	0	0	[16]
173	$C_2O + O \rightleftharpoons CO + CO$	8.32×10^{-11}	0	0	[16]
174	$C_2O + OH \rightleftharpoons CO + CO + H$	3.32×10^{-11}	0	0	[16]
175	$C_2O + O_2 \rightleftharpoons CO + CO + O$	3.32×10^{-11}	0	0	[16]
176	$H_2O_2 + M \rightleftharpoons OH + OH + M$	3.02×10^{-8}	0	42.92	[21]
177	$H_2O_2 + O_2 \rightleftharpoons HO_2 + HO_2$	8.92×10^{-11}	0	39.74	[17]
178	$H_2O_2 + OH \rightleftharpoons H_2O + HO_2$	2.89×10^{-12}	0	0.32	[17]
179	$H_2O_2 + H \rightleftharpoons HO_2 + H_2$	2.82×10^{-12}	0	3.75	[21]
180	$H_2O_2 + H \rightleftharpoons H_2O + OH$	3.98×10^{-11}	0	4.00	[17]
181	$H_2O_2 + O \rightleftharpoons HO_2 + OH$	1.59×10^{-17}	2.0	4.00	[17]
182	$HO_2 + O \rightleftharpoons OH + O_2$	2.89×10^{-11}	0	−0.40	[17]
183	$HO_2 + H \rightleftharpoons OH + OH$	2.82×10^{-10}	0	0.87	[17]
184	$HO_2 + H \rightleftharpoons H_2 + O_2$	1.10×10^{-10}	0	2.13	[17]
185	$HO_2 + H \rightleftharpoons H_2O + O$	5.01×10^{-11}	0	1.72	[21]
186	$HO_2 + OH \rightleftharpoons H_2O + O_2$	2.41×10^{-8}	−1.0	0	[17]
187	$H_2O + M \rightleftharpoons H + OH + M$	5.76×10^{-9}	0	105.20	[21]
188	$H_2O + O \rightleftharpoons OH + OH$	7.59×10^{-15}	1.3	17.10	[17]
189	$H_2O + H \rightleftharpoons H_2 + OH$	7.59×10^{-16}	1.6	19320	[21]
190	$O_2 + M \rightleftharpoons O + O + M$	3.02×10^{-6}	−1.0	118.10	[17]
191	$H_2 + O \rightleftharpoons H + OH$	8.52×10^{-20}	2.7	6.28	[21]
192	$H_2 + M \rightleftharpoons H + H + M$	3.72×10^{-10}	0	96.08	[21]
193	$H + O_2 \rightleftharpoons O + OH$	1.12×10^{-12}	0.6	11.87	[47]
194	$H + O_2 + M \rightleftharpoons HO_2 + M$	1.69×10^{-30}	−0.8	0	[13]
195	$O + H + M \rightleftharpoons OH + M$	1.22×10^{-29}	−1.0	0	[17]
196	$CH + O \rightleftharpoons CHO^+ + e^-$	1.50×10^{-13}	0	0	[48]
197	$CHO^+ + H_2O \rightleftharpoons H_3O^+ + CO$	1.50×10^{-8}	0	0	[49]
198	$H_3O^+ + e^- \rightleftharpoons H_2O + H$	7.60×10^{-2}	−1.6	0	[50, 51]
199	$NaCl + M \rightleftharpoons Na + Cl + M$	8.30×10^{-10}	0	80.0	[52]
200	$Na + M \rightleftharpoons Na^+ + e^- + M$	3.10×10^{-9}	0.5	118.0	[53]
201	$NaCl + M \rightleftharpoons Na^+ + Cl^- + M$	8.20×10^{-2}	−2.0	134.0	[54]
202	$H_3O^+ + Na \rightleftharpoons Na^+ + H_2O + H$	1.10×10^{-8}	0	0	[55]

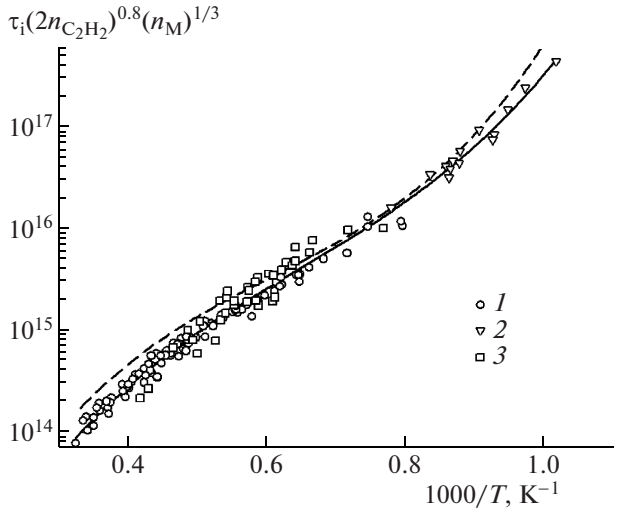

Fig. 5. Ignition delay data for $C_2H_2/O_2/Ar$ mixtures: (*1*) ionization induction period, (*2*) ignition delay data from [6], and (*3*) ignition delay data from [19]. The solid and dashed lines represent the regression analyses of experimental and calculated data, respectively. The τ_i values are in s^{-1}; the $n_{C_2H_2}$ and n_M values, in cm^{-3}.

the C_2H_2 disappearance curve at the inflection point and the initial C_2H_2 concentration line. The dashed third-order curve was obtained by regression analysis of the results of these calculations (the correlation coefficient is 0.996). A comparison between the calculated and experimental relationships suggests that the kinetic scheme reported in [6] provides a good fit for the ignition delay time for acetylene mixtures. At the same time, it leads to somewhat overestimated ignition delay times below 1100 K and above 1600 K.

CONCLUSIONS

The results of the numerical calculations of the ionization kinetics in the oxidation of acetylene and methane [1] provide a qualitative description for the time variation of the electron concentration. This validates the conception of chemical ionization in hydrocarbon flames [3, 4] that is represented as the block of reactions included in Table 2.

Among the hydrocarbon oxidation processes, high-temperature methane oxidation is understood best. Its mechanism has been developed in greatest detail and is widely used in the numerical simulation of various combustion processes. With this mechanism, the results of ionization kinetic calculations coincide with experimental data within the experimental error.

The above-noted differences between the experimental and calculated temperature dependences of electron concentration profile parameters likely arise from the imperfection of the acetylene oxidation scheme. Acetylene oxidation data reported by different authors are often in conflict. Therefore, the process is unstable and depends on external factors that are difficult to take into account. This causes difficulties in numerical simulation. Nevertheless, the calculated ionization kinetics in acetylene oxidation is in satisfactory agreement with experimental data, and the discrepancy between the experimental and calculated acetylene ignition delays can serve as an experimental basis for improvement of the kinetic model of the combustion process.

REFERENCES

1. Karasevich, Yu.K., *Kinet. Katal.*, 2009, vol. 50, no. 1, p. 80 [*Kinet. Catal.* (Engl. Transl.), vol. 50, no. 1, p. 73].
2. Tereza, A.M., Slutskii, V.G., and Severin, E.S., *Khim. Fiz.*, 2003, vol. 22, no. 6, p. 30.
3. Calcotte, H.F., *8th Int. Symp. on Combustion*, Pittsburgh: The Combustion Inst., 1962, p. 184.
4. Miller, M.J., *14th Int. Symp. on Combustion*, Pittsburgh: The Combustion Inst., 1973, p. 307.
5. Karasevich, Yu.K., *Kinet. Katal.*, 2008, vol. 49, no. 5, p. 640 [*Kinet. Catal.* (Engl. Transl.), vol. 49, no. 5, p. 610].
6. Tereza, A.M., Slutskii, V.G., and Severin, E.S., *Khim. Fiz.*, 2009, vol. 28, no. 2, p. 45.
7. Wu, C.H., Singh, H.J., and Kern, R.D., *Int. J. Chem. Kinet.*, 1987, vol. 19, p. 975.
8. Knyazev, V.D. and Slagle, I.R., *J. Phys. Chem.*, 1996, vol. 100, p. 16899.
9. Marinov, N.M., Pitz, W.J., Westbrook, C.K., Vincitore, A.M., Castaldi, M.J., and Senkan, S.M., *Combust. Flame*, 1998, vol. 114, p. 192.
10. Wang, H. and Frenklach, M., *Combust. Flame*, 1997, vol. 110, p. 173.
11. Hidaka, Y., Nishimori, T., Sato, K., Henmi, Y., Okuda, R., and Inami, K., *Combust. Flame*, 1999, vol. 117, p. 755.
12. Laufer, A.H. and Fahr, A., *Chem. Rev.*, 2004, vol. 104, p. 2813.
13. Baulch, D.L., Cobos, C.J., Cox, R.A., et al., *J. Phys. Chem. Ref. Data*, 1994, vol. 23, p. 847.
14. Dean, A.M., *J. Phys. Chem.*, 1985, vol. 89, p. 4600.
15. Diau, E.W. and Lin, M.C., *J. Chem. Phys.*, 1994, vol. 101, p. 3923.
16. Eiteneer, B. and Frenklach, M., *Int. J. Chem. Kinet.*, 2003, vol. 35, no. 9, p. 391.
17. Tsang, W. and Hampson, R.F., *J. Phys. Chem. Ref. Data*, 1986, vol. 15, p. 1087.
18. Laskin, A. and Wang, H., *Chem. Phys. Lett.*, 1999, vol. 303, p. 43.
19. Miller, J.A. and Melius, C.F., *22nd Int. Symp. on Combustion*, Pittsburgh: The Combustion Inst.,1989, vol. 22, p. 1031.
20. Woods, I.T. and Haynes, B.S., *25th Int. Symp. on Combustion*, Pittsburgh: The Combustion Inst.,1994, p. 909.
21. Baulch, D.L., Cobos, C.J., Cox, R.A., et al., *J. Phys. Chem. Ref. Data*, 1992, vol. 21, p. 411.

22. Frank, P. and Just, Th., *Proc. Int. Symp. Shock Tubes Waves,* Sydney, 1984, vol. 14, p. 706.
23. Knyazev, V.D., Stoliarov, S.I., and Slagle, I.R., *26th Int. Symp. on Combustion*, Pittsburgh: The Combustion Inst.,1996, p. 513.
24. Bartels, M., Edelbuttel-Einhaus, J., and Hoyermann, K., *23rd Int. Symp. on Combustion*, Pittsburgh: The Combustion Inst.,1990, p. 131.
25. Frank, P., Bhaskaran, K.A., and Just, Th., *J. Phys. Chem.*, 1986, vol. 90, p. 2226.
26. Hidaka, Y., Hattori, K., Okuno, T., Inami, K., Abe, T., and Koike, T., *Combust. Flame*, 1996, vol. 107, p. 401.
27. Frank, P., Bhaskaran, K.A., and Just, Th., *21st Int. Symp. on Combustion*, Pittsburgh: The Combustion Inst.,1988, p. 885.
28. Glarborg, F., Miller, J.A., and Kee, R.J., *Combust. Flame*, 1986, vol. 65, p. 177.
29. Peeters, J., Boullart, W., and Devriendt, K., *J. Phys. Chem.*, 1995, vol. 99, p. 3583.
30. Dombrowsky, Ch., Hoffmann, A., Klatt, M., and Wagner, H.Gg., *Ber. Bunsen-Ges. Phys. Chem.*, 1991, vol. 95, p. 1685.
31. Li, S.C. and Williams, F.A., *26th Int. Symp. on Combustion*, Pittsburgh: The Combustion Inst.,1996, p. 1017.
32. Grotheer, H.H. and Just, Th., *Chem. Phys. Lett.*, 1981, vol. 78, p. 71.
33. Olsson, J.M., Olsson, I.B.M., and Andersson, L.L., *J. Phys. Chem.*, 1987, vol. 91, p. 4160.
34. Troe, J., *J. Phys. Chem. A*, 2005, vol. 109, p. 8320.
35. Hsu, C.C., Mebel, A.M., and Lin, M.C., *J. Chem. Phys.*, 1996, vol. 105, p. 2346.
36. Bozzelli, J.W. and Dean, A.M., *J. Phys. Chem.*, 1990, vol. 94, p. 3313.
37. Markus, M.W., Woiki, D., and Roth, P., *24th Int. Symp. on Combustion*, Pittsburgh: The Combustion Inst.,1992, p. 581.
38. Rohrig, M., Petersen, E.L., Davidson, D.F., Hanson, R.K., and Bowman, C.T., *Int. J. Chem. Kinet.*, 1997, vol. 29, no. 4, p. 781.
39. Bauerle, S., Klatt, M., and Wagner, H.Gg., *Ber. Bunsen-Ges. Phys. Chem.*, 1995, vol. 99, p. 870.
40. Markus, M.W., Roth, P., and Tereza, A.M., *25th Int. Symp. on Combustion*, Pittsburgh: The Combustion Inst.,1994, p. 705.
41. Dombrowsky, Ch. and Wagner, H.Gg., *Ber. Bunsen-Ges. Phys. Chem.*, 1992, vol. 96, p. 1048.
42. Dombrowsky, Ch., Hwang, S.M., Rohrig, M., and Wagner, H.Gg., *Ber. Bunsen-Ges. Phys. Chem.*, 1992, vol. 96, p. 194.
43. Harding, L.B., Guadagnini, R., and Schatz, G.C., *J. Phys. Chem.*, 1993, vol. 97, p. 5472.
44. Lichtin, D.A., Berman, M.R., and Lin, M.C., *Chem. Phys. Lett.,* 1984, vol. 108, p. 18.
45. Jachimowski, C.J., *Combust. Flame*, 1977, vol. 29, no. 1, p. 55.
46. Miller, J.A. and Garrett, B.C., *Int. J. Chem. Kinet.*, 1997, vol. 29, p. 275.
47. Burcat, A. and McBride, B., *1997 Ideal Gas Thermodynamic Data for Combustion and Air Pollution Use*, Technion Aerospace Engineering Report no. 804, Haifa, 1997.
48. Peeters, J. and Vinckier, C., *15th Int. Symp. on Combustion*, Pittsburgh: The Combustion Inst.,1974, p. 969.
49. Aravin, G.S., Vlasov, P.A., Karasevich, Yu.K., Makolkin, E.V., and Neigauz, M.G., *Fiz. Goreniya Vzryva*, 1982, no. 1, p. 49.
50. Hayhurst, A.N. and Telford, N.R., *J. Chem. Soc., Faraday Trans. 1*, 1974, no. 11, p. 181.
51. Kelly, R. and Padly, P.J., *Trans. Faraday Soc.*, 1970, vol. 66, no. 5, p. 1127.
52. Hartig, R., Olschewski, H.A., Troe, J., and Wagner, H.Gg., *Ber. Bunsen-Ges. Phys. Chem.*, 1968, vol. 72, no. 8, p. 1016.
53. Bates, D.R., *Proc. R. Soc. London, Ser. A*, 1976, vol. 348, no. 1655, p. 427.
54. Schneider, K.P. and Park, C., *Phys. Fluids*, 1975, vol. 18, no. 5, p. 969.
55. Hayhurst, N.A. and Sugden, T.M., *Proc. R. Soc. London, Ser. A*, 1966, vol. 293, no. 1600, p. 36.
56. Tsang, W., *J. Phys. Chem. Ref. Data*, 1987, vol. 16, p. 471.
57. Kistiakowsky, G.B. and Richards, L.W., *J. Chem. Phys.,* 1962, vol. 36, p. 1707.